Journal of Polymers and the Environment (2018) 26:3176–3186
https://doi.org/10.1007/s10924-018-1205-8

ORIGINAL PAPER

Effect of Hydrothermal Aging on Injection Molded Short Jute Fiber Reinforced Poly(Lactic Acid) (PLA) Composites

Ning Jiang[1] · **Tao Yu**[1,2,3] · **Yan Li**[1]

Abstract

This work focused on the durability of short jute fiber reinforced poly(lactic acid) (PLA) composites in distilled water at different temperatures (23, 37.8 and 60 °C). Morphological, thermal and mechanical properties (tensile, flexural, and impact) of jute/PLA composites were investigated before and after aging. Different from traditional synthetic fiber reinforced polymer composites, the stability of jute/PLA composites in water was significantly influenced by hydrothermal temperature. The mechanical properties of the composites and molecular weight of PLA matrix declined quickly at 60 °C, however, this process was quite slower at temperatures of 23 and 37.8 °C. Impact properties of the composites were hardly decreased, but the tensile and flexural properties suffered a drop though to various degrees with three degradation stages at 23 and 37.8 °C. The poor interface of composites and the degradation of PLA matrix were the main damage mechanism induced by hydrothermal aging. Furthermore, considering the hydrolysis of PLA matrix, the cleavage of PLA molecular chain in different aging time was quantitatively investigated for the first time to illustrate hydrolysis degree of PLA matrix at different aging time.

Keywords Short plant fibers · Injection molding · Hydrothermal aging · Thermal properties · Aging mechanism

Introduction

The current energy shortage and environmental pollution have received people's attention to green and sustainable materials. It is one of most important methods by using green biodegradable materials instead of petroleum-based plastics to reduce the damage of environment. Poly(lactic acid) (PLA), as a green material, is available from crop starch, and its process of production requires less fossil resources as compared to petroleum-based plastics [1–5]. In addition, PLA also has good properties such as high stiffness, compatibility and clarity to partly replacing petroleum-based plastics [6, 7]. Recently, plant fibers have gained attention to replace conventional synthetic fibers as reinforcement in polymer matrices to design material due to their high specific strength and modulus, low density, low cost, good recyclable and degradable properties [8–14]. Now, plant fiber reinforced PLA composites are trying to use in automotive industry for their good biodegradation and high-modulus [15, 16]. However, due to the hygroscopic nature of the fibers and biodegradable characteristics of PLA, adverse effects of aging may occur, which influence the service life of plant fiber reinforced PLA composites [17]. Therefore, it is necessary to research their aging behaviors for the applications.

Nature aging tests are very representative but extremely time-consuming [18]. As an accelerated degradation process, hydrothermal aging can be used to investigate the aging behaviors in a short period [19]. Many literatures focused on the hydrolytic degradation of PLA [20–23]. Gorrasi et al. [24] have studied the hydrolysis process of different commercial grades of PLA. It was found that the amorphous sample following a higher hydrolysis rate compared to the crystalline one. For the crystalline PLA, Andersson et al. [22] reported that the hydrolysis of chains proceed

✉ Tao Yu
yutao@tongji.edu.cn

✉ Yan Li
liyan@tongji.edu.cn

[1] School of Aerospace Engineering and Applied Mechanics, Tongji University, 1239 Siping Road, Shanghai 200092, People's Republic of China

[2] State Key Laboratory of Molecular Engineering of Polymers, Fudan University, Shanghai 200433, People's Republic of China

[3] State Key Laboratory for Strength and Vibration of Mechanical Structures, Xi'an Jiaotong University, Xi'an 710049, People's Republic of China

preferentially in the amorphous regions due to its poor water resistance. However, the hydrothermal aging process of plant fiber/PLA composite is different from that of neat PLA due to the addition of plant fiber. Firstly, plant fiber can enhance the water absorption of plant fiber/PLA composites compared to neat PLA for owing large number of lumens [13, 25, 26]. Moreover, the fiber can affect the crystallinity of PLA, and then its aging. Ndazi et al. [27] found that the rice hulls can bring more defects to decrease the crystallinity of PLA matrix which also promoted the aging of composites. On the contrary, Spiridon et al. [28] stated the crystallinity of PLA increased after adding lignin. The different crystallinity of PLA was determined by the size and form of plant fiber in the composites. Furthermore, the manufacturing method is also very important. Sreekumar et al. [29] showed that the weight gain of sisal fiber reinforced polyester composites made by resin transfer molding (RTM) was lower than hot pressed one, since the lower internal stress and less porosity in composites produced by RTM. Meanwhile, the water absorption, mechanical properties and microstructure evolution of hot pressed wood fiber [30, 31], lignin [28] and short jute fiber [13] reinforced PLA composites were investigated after aging. However, in automotive industry, in order to improve the production and efficiency, the parts of the automobile were usually produced by injection molding. The crystal, the size and form of plant fiber, the interface between plant fibers and PLA matrix of injection molded composites are different from that of hot pressed composites, which may make the different aging behaviors of plant fiber/PLA between two molding methods.

Related to the other works on plant fiber/PLA composites, to our knowledge, few results have been put forward so far regarding the aging behavior of injection molded short plant fiber/PLA composites to hydrothermal environment. Regazzi et al. [32] studied the aging of injection molded flax fiber/PLA composites. Srubar et al. [33] and Almgren et al. [30] have researched the influence of moisture on the morphological and mechanical properties of wood fiber composites. However, the microstructures of jute fiber in our study differ from those of flax fiber [34] and wood fiber, which may lead to the different aging mechanism [32]. For example, the lignin content of jute fiber, flax fibers and wood fibers are 17, < 3 and 10–20% respectively, which can influence the water absorption of fiber and adhesion between the matrix and fibers [35]. In addition, the effects of short plant fiber on the hydrolysis degradation of PLA matrix, for example, the change of crystallinity and the molecular chain movement of PLA are still not clearly understand. It is necessary to study the aging of the injection molded short jute fiber/PLA composites to facilitate its applications.

In this work, the effect of hydrothermal aging on the water absorption, thermal and mechanical properties of injection molded short jute fiber/PLA composites at three different temperatures (23, 37.8 and 60 °C) were investigated. Differential scanning calorimetry (DSC), gel permeation chromatography (GPC), scanning electronic microscopy (SEM) were used to characterize the prepared jute/PLA composites to analyse their aging mechanism. The cleavages of PLA molecular chains were also analyzed at different aging time to illustrate hydrolysis degree of PLA matrix.

Materials and Methods

Materials

Poly(lactic acid) (PLA) (4032D, M_w = 150,000, D stereoisomer content of about 1.5%) was obtained from Suzhou Jiwang Environmentally Friendly Material Co. Ltd. Jute fiber yarn was purchased by Shanghai Qiancong Jute Fiber Co. Ltd., China.

Composites Preparation

Prior to processing, jute fibers and PLA were dried under vacuum at 80 °C for 4 h. Then the dried jute fibers and PLA were blended by using a SHJ-20 twin-screw extruder with a 27 mm screw diameter (L/D = 40, Nanjing Jieya Co. Ltd, China). The extrusion temperature was independently controlled at eight zones 150, 160, 165, 170, 175, 175, 165 and 155 °C from feed zone to exit die and a screw speed setting of 150 rpm. The residence time was approximately 60 s and the weight percent of jute fibers was 10%. The diameter of jute fiber was 30–50 µm, and the average length was about 2.5 mm in the composites. The jute/PLA composites were granulated and dried under vacuum at 80 °C for 4 h. Finally, the composites were molded into mechanical test specimens using an injection molding machine with a barrel temperature of 175 °C.

Water Absorption

The water absorption test samples with dimensions $30 \times 20 \times 4$ mm^3 were dried in a vacuum oven at 60 °C for 4 h prior to immerse in water. Each sample was weighed as initial mass (W_0) and then set in the deionized water baths at 23, 37.8 and 60 °C, respectively. Weight gain (W_t) was measured by periodic weighting five samples. The water absorption (%) (M_t) was calculated by the Eq. (1):

$$M_t = \frac{W_t - W_0}{W_0} \times 100 \tag{1}$$

In the first stage, the water absorption was controlled by diffusion. If the water absorption follows Fick's law of diffusion, the weight gain can be expressed in term of two parameters, namely, the diffusion coefficient (D) and maximum moisture content (M_m) as in Eq. (2) [36].

$$\frac{M_t}{M_m} = \frac{4}{h}\left(\frac{D}{\pi}\right)^{1/2} \times \ t^{1/2} \tag{2}$$

where h is the thickness of the specimen, and t is the time. The diffusion coefficient (D) can be calculated by Eq. (3) from the slope (k) of the initial linear portion of the absorption curve.

$$D = \pi\left(\frac{kh}{4M_m}\right)^2 \tag{3}$$

The composite is considered to be the isotropic material due to the random distribution of short fibers. So the D_x can be expressed as [37]:

$$D_x = D\left(1 + \frac{h}{l} + \frac{h}{n}\right)^{-2} \tag{4}$$

where D_x is the diffusion coefficient of the composites in thickness direction. l and n are the length and width of sample respectively.

Scanning Electron Microscopy (SEM)

The morphologies of composites fracture surfaces of the impact test samples were recorded and analysed by a scanning electron microscope (SEM) (Quanta 250 FEG, FEI Ltd., USA). Prior to SEM observations, the samples were dried 24 h at room temperature. Then the samples were covered with gold using a vacuum sputter coater and observed at a voltage of 15 kV.

Differential Scanning Calorimetry (DSC)

Differential scanning calorimetry (DSC) measurement was carried out by a Q20 thermal analysis system (TA, USA). The simples (4–5 mg) were heated from 20 to 200 °C at 10 °C/min. Glass transition temperature (T_g), cold crystallization temperature (T_c) and Melting temperature (T_m) were estimated based on the DSC scan. Crystallinity degree (χ%) was calculated by the Eq. (4):

$$\chi\ (\%) \ = \ \frac{\Delta H_m - \Delta H_c}{\Delta {H_m}^0 \ \times \ (1 - \Phi_{JF})} \ \times \ 100\% \tag{4}$$

where ΔH_c, ΔH_m and $\Delta {H_m}^0$ are the enthalpies of cold crystallization, melting and melting of fully crystalline PLA, which can be found in the literature to be 93.1 J/g [38]. Φ_{JF} is the content of jute fiber in jute/PLA composites.

Gel Permeation Chromatography (GPC)

The molecular weight of PLA before and after degradation was measure by gel permeation chtomatography (GPC) on a P320 system (Yilite, China). The samples were prepared with 10 mg from a layer in the middle of the aging material. Then it was dissolved into 10 ml chloroform solvent for 2 h. After filtration, the samples were transferred into 2 ml vials for analysis.

Calculation of Molecular Cleavage

The average number of cleavages per PLA molecule, $N_{\text{cleavages}}$, can be calculated by the Eq. (5).

$$N_{cleavages} = \frac{DP_O}{DP_t} - 1 \tag{5}$$

where DP_o and DP_t are the degree of polymerization of PLA before and after aging time t, respectively. Which can be also written as

$$N_{cleavages} = \frac{n}{n_t} - 1 \tag{6}$$

where n and n_t are the value of constitutional unit of PLA before and after aging time t, respectively. The value of the degree of polymerization (DP) was equal to the value of constitutional unit (n), which can be calculated by molecular weights of PLA.

Mechanical Properties Measurement

The tensile and flexural properties were measured on a WHY-W machine (Chengde instruments Ltd., China). The tensile testing was performed according to ASTM D3039 standard and the crosshead speed was 2 mm/min. The flexural testing at a crosshead speed of 2 mm/min and a span of 64 mm was determined according to ASTM D790, and the size of flexural testing samples was 80 × 10 × 4 mm^3. The impact strength was tested according to GB/T 1843 using a XCJ-50 test machine (Chengde test instrument Ltd., China). The size of impact testing samples was 80 × 10 × 4 mm^3.

Results and Discussion

Water Absorption

Figure 1 shows the percentage of weight gain rate (M_t) as function of square root of the time ($\text{day}^{1/2}$) for jute/PLA composite samples at 23, 37.8 and 60 °C, respectively. Water absorption of jute/PLA composites showed only two distinct

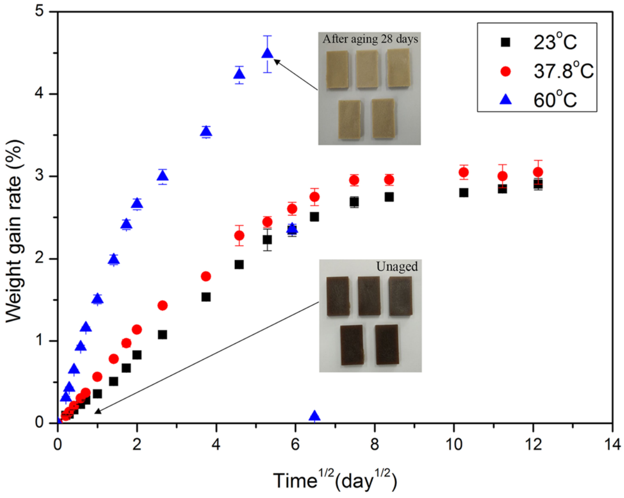

Fig. 1 The weight gain rate (M_t) in function of the square root of the time. Optical images of the sample at 60 °C were also reported

stages at 23 and 37.8 °C, but three stages at 60 °C. A rapid water absorption of all jute/PLA composites were found in first few days. There was a linear relationship between M_t and $t^{1/2}$ at the beginning, which indicated that the water absorption of jute/PLA composites at three temperatures followed Fickian behavior in the first stage. There was no irreversible physical change or chemical reaction, and water molecular just diffused from high to low concentration along jute fiber, PLA matrix and interface. Then the M_t reached saturation and keep equilibrium at 23 and 37.8 °C. The change of M_t of jute/PLA composites at 23 and 37.8 °C was similar with the pure PLA reported by Ndazi et al. [27]. However, aged at 60 °C, the experimental data deviated from the Fickian law, for M_t increased again after aging 14 days without an equilibrium, which was quite different from M_t of pure PLA at 58 °C (above T_g) [39] and flax/PLA composites at temperatures below T_g [32]. The pure PLA without jute fibers has a slow water absorption with an equilibrium, which different from jute/PLA composites. It was attributed to capillarity of microcracks and microvoid caused by swelling of fibers [17], which promoted the water absorption of jute/PLA composites. Meanwhile, the high temperature (above T_g) accelerated the hydrolysis of PLA contributed to the growth of crack, which also increased the water absorption of jute/PLA composites. It made the M_t increased again compared to flax/PLA composites at temperatures below T_g [32]. The poor interface and the emergence of crack in PLA matrix could be proved in Fig. 2b. The good interfacial bonding was found in unaged composites, and no crack was observed in the matrix (Fig. 2a). Interesting to note that, after reaching the maximum of water absorption, the specimens at 60 °C had a significant weight loss due to the degradation of composites, which led to the increase of cracks (Fig. 2c). The hydrolysed short water-soluble fragments of PLA and the exfoliated jute fiber from the surface of composite into water lead to the decrease of the M_t. Figure 1 revealed the jute/PLA composites immersed at 60 °C became white after the 28 days, which was due to that the water the water went inside the material, and formed lots of micro cracks. That could affect the reflection and refraction of light, which makes the color of the composites turn into white consequently.

The M_m and D_x values are evaluated and summarized in Table 1. By comparing M_m and D_x of composites aged at different conditions, it can be observed that temperature showed a significant effect on water absorption. Both the saturation level and diffusivity increased with the increasing temperature. The diffusion coefficients of jute/PLA composites at 23 °C ($D = 6.72 \times 10^{-13}$ m^2/s), at 37 °C ($D = 9.00 \times 10^{-13}$ m^2/s) and at 60 °C ($D = 18.90 \times 10^{-13}$ m^2/s) suggested a thermal rate dependency. A similar trend was found in 10% lignocellulose/polypropylene (PP) composites at different temperatures (23, 50 and 70 °C), where the diffusion coefficient increased from 1.67 to 16.5×10^{-13} m^2/s

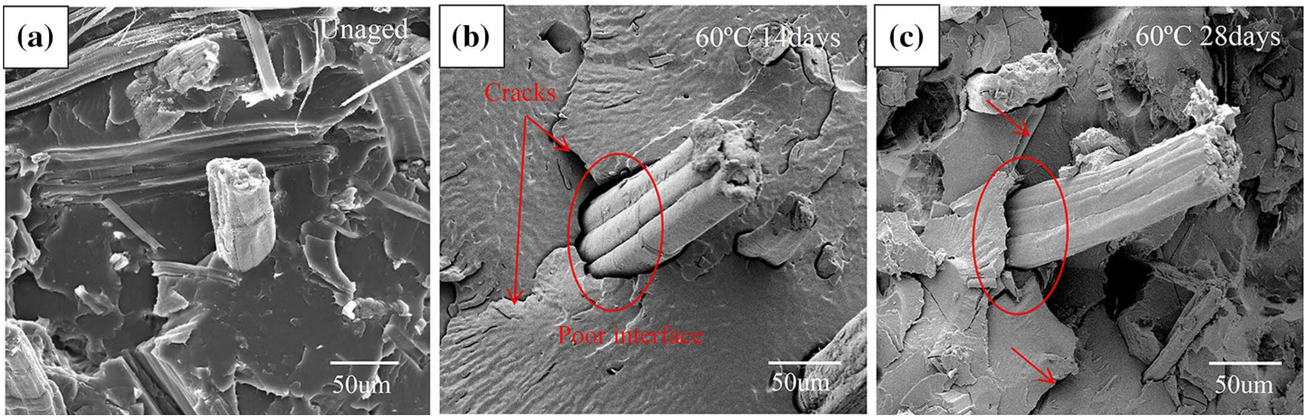

Fig. 2 SEM image of the fracture surfaces of jute/PLA composite, **a** before aging, **b** aging 14 days, **c** aging 28 days at 60 ºC

Table 1 Fickian diffusion coefficients of jute/PLA composites at 23, 37.8 and 60 °C

Temperature (°C)	h(m)	k	M_m (%)	D_x ($\times 10^{-13}$ m^2/s)
23	0.004	0.00170	2.75	6.72
37.8	0.004	0.00216	2.96	9.00
60	0.004	0.00446	4.31	18.90

[40]. Srubar et al. [41] also reported values of 5.82 and 13.65×10^{-13} m^2/s for polyolefin matrices reinforced with weight fractions of 40% wood fiber at 4 and 37 °C, respectively. In addition, the M_m of plant fiber/PLA composites was apparently higher than that of pure PLA at the same aging temperature [27, 39]. This was related to hydroxyl and lumen of jute fiber, which can promote water absorption.

Thermal Properties and Crystallinity

By differential scanning calorimetry (DSC), the thermal properties and crystallinity have been investigated to further study the effect of jute fiber on the hydrolysis of PLA. Figure 3 shows the heating DSC curves of the samples at three temperatures, it can be found that the high temperature (above T_g) has a strong influence on the thermal properties of the composites. Cold crystalline disappeared and melting endotherm increased for the samples after aging at 60 °C, which was attributed to the improved crystalline capacity of PLA chains at high temperature. With the increase of aging time, the T_g almost disappeared at 60 °C. It may be due to the increased crystallinity, which limited the movement of PLA molecular chains.

A summary of DSC results from DSC scan was reported in Fig. 4. The change of T_g at 23 and 37.8 °C showed three stages (Fig. 4a). At the first stage, there was a decline in T_g due to the enhanced chain mobility induced by the plasticizing effect of water molecules. Then the increase of crystallinity enhanced the T_g by limit the chain mobility. The decrease of molecular weight resulted in the second decline of T_g. In contrast, T_g continue to rise with increasing time then disappeared at 60 °C. This was attributed to the increase of crystallinity which improved the regularity of molecular chain.

The melt temperature of jute/PLA composite at 23 and 37.8 °C initially shift to high temperature then declined (Fig. 4b). The initial increase occurred in the period from 0 to 120 days, which was due to the formation of thicker crystals [42]. With the hydrolysis continued, the PLA chain in crystalline region began to hydrolyse due to bulk erosion. It induced a reduction in the melt temperature of the sample. There was a similar trend in the melt temperature at 60 °C,

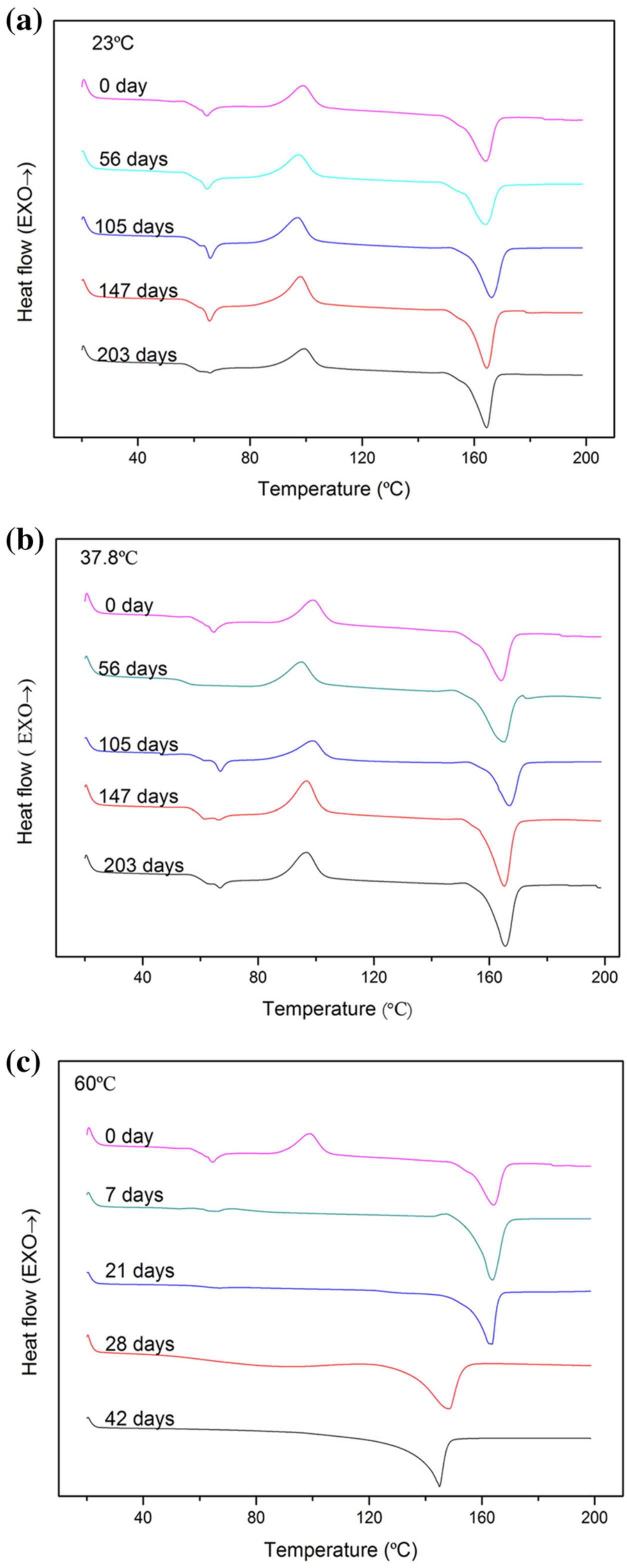

Fig. 3 DSC thermograms of jute/PLA composites before and after aging at **a** 23, **b** 37.8, **c** 60 °C

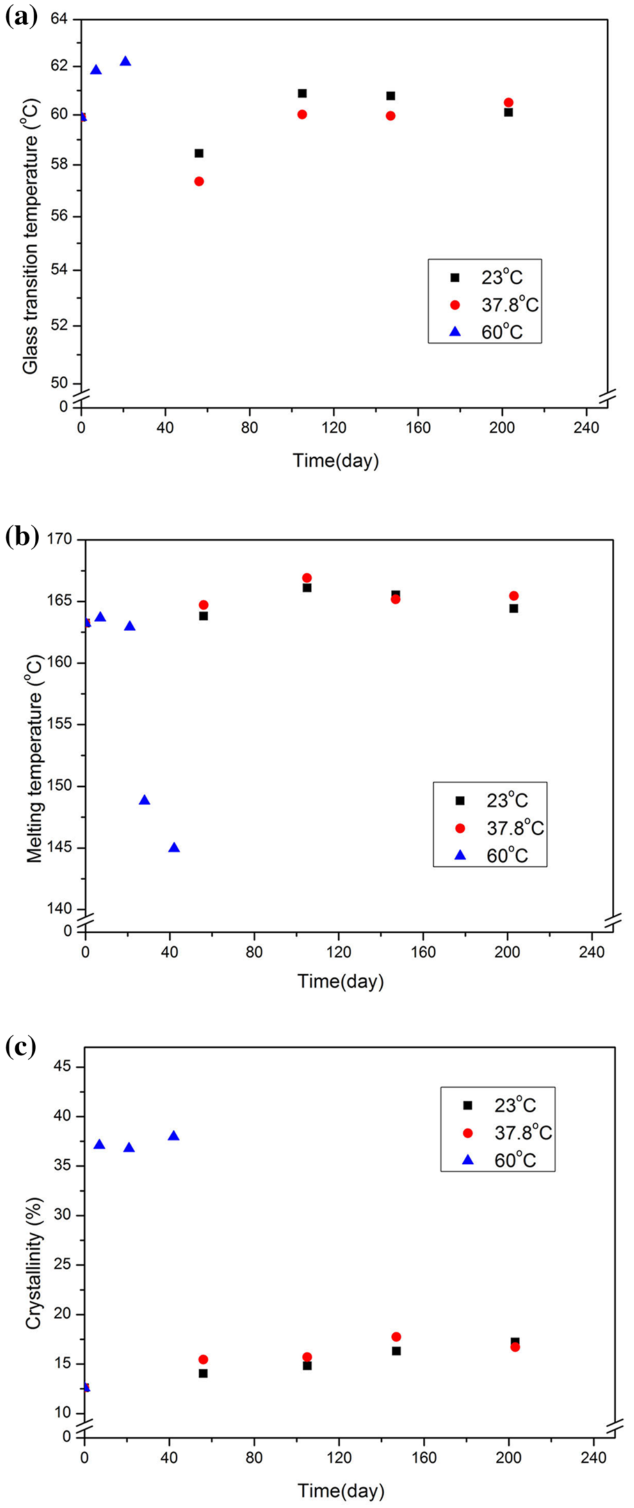

Fig. 4 Summary of DSC results: **a** glass transition temperature, **b** melting temperature, **c** crystallinity

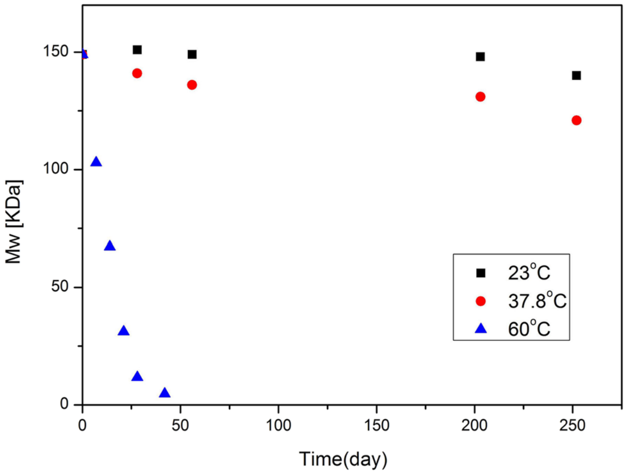

Fig. 5 Weight average molecular weight changes during the aging of PLA at 23, 37.8 and 60 °C

however, the decline was more quickly which was ascribed to the decrease of molecular weight.

Figure 4c shows the crystallinity obtained from the DSC results. There was similar change in the crystallinity of the composite at 23 and 37.8 °C. At first stage, hydrolysed less than 70 days, no obvious change in the crystallinity can be observed. It can be explained that the time was too short for the chain segment mobility to crystallize. At 60 °C, the crystallinity of samples showed an evident increase from 15.47 to 37.88% after 7 days aging. This was due to the addition of short jute fiber which serves as nucleating agent leading to increase the crystallinity of PLA during aging. The results were opposite to hot press molded plant fiber/PLA composites, which have a decrease of PLA matrix crystallinity during aging [27]. The difference could be explained that the longer size and non-uniform distribution of plant fiber in the hot press molded composites can bring more defects to decrease the crystallinity of PLA matrix.

Molecular Weight Analysis

In order to analyze the degree of PLA hydrolysis, molecular weight was tested by GPC. Figure 5 shows the results of molecular weights (M_w) analysis of PLA before and after aging at 23, 37.8 and 60 °C. The M_w decreased slowly at 23 and 37.8 °C, while it reduced very quickly at 60 °C. This indicated that the rate of PLA hydrolysis was strongly temperature dependent. The higher temperature (above T_g) accelerated the hydrolytic degradation of PLA. At the second stage, the emergence of an obvious descend of M_w at 23 and 37.8 °C compared to M_w at the first stage. However, starting from the early stage of aging at 60 °C, there was a rapid decline of M_w which was quite faster than that at 50 °C studied by Regazzi [32]. The fast decline may be due to the

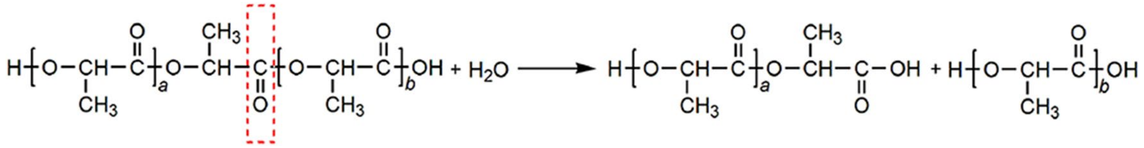

Fig. 6 Hydrolysis mechanism of PLA

Table 2 The average number of cleavages per PLA molecule at 23, 37.8 and 60 °C after different aging time

Temperature (°C)	Aging time(days)						
	7	14	21	28	42	70	252
23	–	–	–	–	–	0.006	0.064
37.8	–	–	–	–	–	0.095	0.231
60	0.447	1.218	3.793	11.753	30.751		

accelerated movement of molecular chain and auto-catalytic when aging temperature above T_g. The value of M_w declined from 149,000 to 103,000 at 60 °C after aging 7 days. While after aging 42 days, only about 4710 left. In order to further analyse the aging of the PLA, the average number of cleavages per PLA molecule would be calculated.

The hydrolysis of PLA occurs by random cleavage of –C–O– ester bond by water molecules. In Fig. 6, the hydrolysis mechanism of PLA was presented.

The $N_{cleavages}$ of PLA at 23, 37.8 and 60 °C after different aging time were presented in Table 2. The changes of $N_{cleavages}$ at 23 and 37.8 °C were much less than that at 60 °C. After 70 days, the $N_{cleavages}$ at 23 and 37.8 °C were 0.006 and 0.095, respectively, which meant average among each 1000 PLA chains, there were about 6 cleavages at 23 °C and 95 cleavages at 37.8 °C. The $N_{cleavages}$ of PLA had an obvious increase over aging time. After 252 day, the $N_{cleavages}$ of PLA increased to 0.064 and 0.231 at 23 and 37.8 °C, respectively. The increase of $N_{cleavages}$ indicated the degradation of jute/PLA composites. However, at 60 °C, greatly significant increase in the $N_{cleavages}$ of PLA was noted. After 42 days, the $N_{cleavages}$ can reach 30.751 which meant average among each PLA chains, there were about 30.751 cleavages. It elucidated that the rate of PLA hydrolysis was strongly temperature dependent. The higher temperature (above T_g) accelerated the hydrolytic degradation of PLA. According to the data fitting, it can be checked that the relationship between $N_{cleavages}$ and aging time was a quadratic formula, which indicated that the polyester undergo an auto-catalytic during hydrolysis as a result of acceleration by their carboxylic end groups.

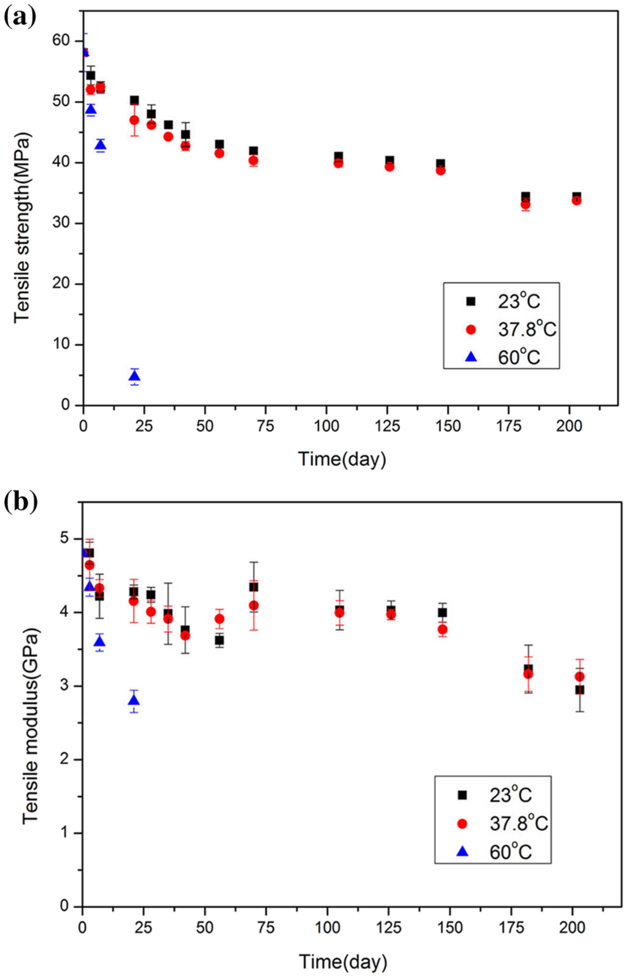

Fig. 7 The tensile properties of jute/PLA composite before and after aging. **a** Tensile strength. **b** Tensile modules

Mechanical Properties

The aging behavior of jute/PLA composites in hydrothermal environment can bring the change of mechanical properties. The tensile strength and tensile modulus of jute/PLA composites before and after aging at 23, 37.8 and 60 °C were presented in Fig. 7. There were three stages of tensile properties at 23 and 37.8 °C. From Fig. 7, it can be seen that tensile strength showed a remarkable decrease at beginning of aging, then stabilized for a period of time and decreased at last. The first decrease in tensile properties was caused by the poor interface between jute fiber and PLA matrix [43]. It could be proved in Fig. 8, there were micro-cracks at the fiber/matrix interface after aging 56 days at 23 and 37.8 °C. The decline of tensile properties was due to large number of hydroxyl and lumens in jute fiber, which promoted the water absorption. There was swelling of jute fiber, which can lead to the stress in composites [44]. The stress would accelerate the debonding process, resulting in the worse interface between jute fiber and PLA matrix, which also lead to the decline in tensile strength and modulus. At the second stage, tensile strength remained constant and the tensile modulus also keep stable after slightly increased, which was due to the increase of crystallinity. Water absorption during aging at low temperatures (less than T_g) act as an effective plasticizer, increasing the aggregation of PLA chains and promoted nucleation and crystallization of the PLA molecules [45], which was proved by DSC results. The enhanced crystallinity can improve the regularity of molecular chain, which can increase the mechanical properties. However, the tensile strength and tensile modulus declined again after 147 days. This decline was due to the decrease of PLA molecular weight by hydrolysis, which meant the cleavage of the molecular chain. The decrease of PLA molecular was proved by the results of GPC. After aging 203 days at 23 °C in distilled water, a few numbers of voids can be observed in the matrix and the interface between fiber and matrix further was deteriorated due to the hydrolysis of PLA matrix (Fig. 8). The composites at 37.8 °C were in the same situation.

The tensile strength and modulus decreased very quickly at 60 °C. As shown in Fig. 7, after aging 7 days, the tensile strength and tensile modulus of jute/PLA composites quickly declined 27.59 and 25.28%, respectively. The tensile properties of jute/PLA composite were difficult to measure after 21 days, which was due to the very brittle nature of the aged

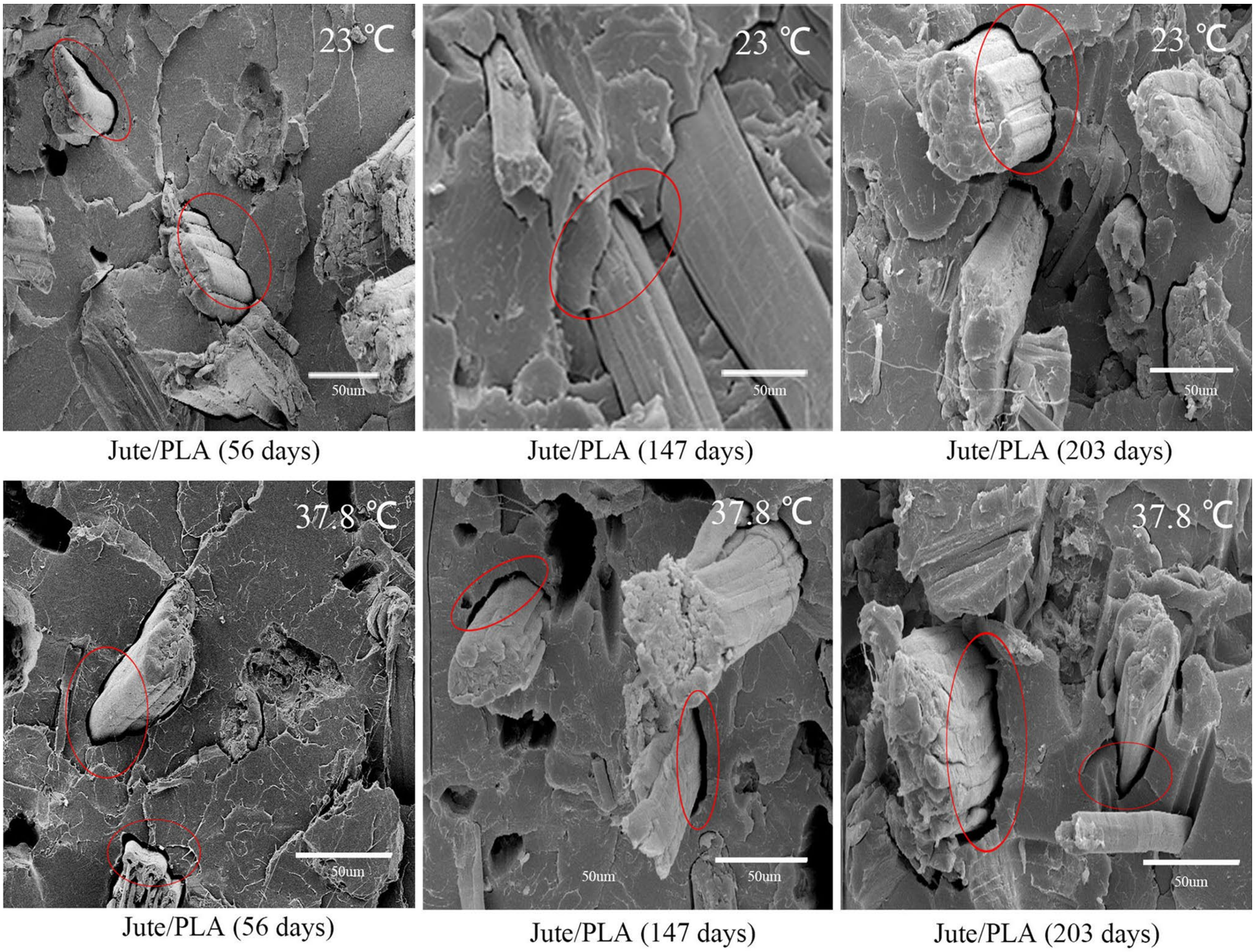

Fig. 8 SEM image of the fracture surfaces of jute/PLA composite after different aging time at 23 and 37.8 °C

specimens. The main reason of rapid decline of the tensile strength and modulus at 60 °C was the degradation of PLA by the hydrolysis. The high temperature made the active molecular motion which facilitated the diffusivity of water into PLA matrix. Then PLA had a drastic degradation, and there was crack on matrix, which can be observed in Fig. 2c. The decrease of tensile strength was more quickly in hot press molded plant fiber/PLA for the more water absorption. In addition, the degradation of jute fiber was another reason for the decreased mechanical properties of the jute/PLA composites. It could be inferred that pectins, lignin, hemicellulose and some poorly crystallized cellulose in jute fibers hydrolyzed. Thuault et al. [46] stated that water could seep into the fiber and disorganized the microfibrils network, which brought to a decrease of the fiber strength.

Figure 9 shows the flexural strength and flexural modulus of jute/PLA composites before and after aging at three temperatures. It was found that flexural strength and modulus of jute/PLA composites decreased with hydrothermal aging. These results have a similar trend with tensile properties of the composites. Note that flexural modulus of jute/PLA composites at 60 °C showed an increase after 7 days aging which was due to the increased crystallinity.

The impact strength results of jute/PLA composite at different hydrolysis temperature were shown in Fig. 10. There was no significant change in impact strength at 23 and 37.8 °C. The impact strength had a small increase until aging 48 days which was attributed to the enhanced chain mobility induced by the plasticizing effect of water molecules. Then it declined due to the poor interface. A cushion caused by voids and water gave rise to the second increase in the impact strength. After aging 150 days, the impact strength of jute/PLA composites at 23 and 37.8 °C declined again which was ascribed to the degradation of PLA matrix. For the composites at 60 °C, the impact strength had an increase then declined quickly. The plasticizing effect of water molecules and the cushion caused by water and voids lead to the increase of impact strength. After aging 7 days, the worse interface and the degradation of PLA lead to the rapid decline of impact strength at 60 °C. Moreover, the increase of crystallinity also declined the impact strength, which was attributed to limited chain mobility.

Hydrothermal Aging Mechanism Analysis

According to analysis of weight gain rate, morphological, thermal and mechanical properties and molecular weight of jute/PLA composites before and after aging, the hydrothermal aging mechanisms of jute/PLA were summarized in Fig. 11. In first stage, the water diffused into the jute/PLA composites through matrix and the lumen of jute fiber. There was the swelling of jute fiber due to existence of moisture. The different expansion of jute fiber and

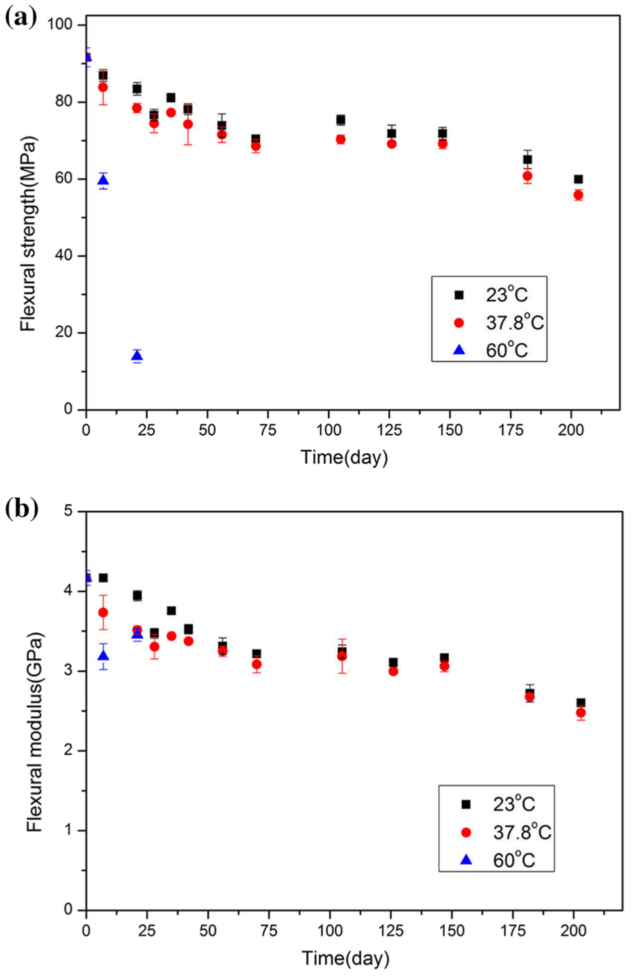

Fig. 9 The flexural properties of jute/PLA composite before and after aging. **a** Flexural strength. **b** Flexural modulus

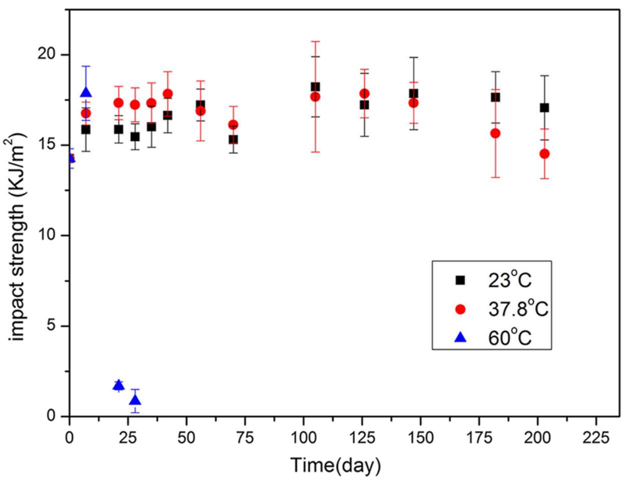

Fig. 10 The impact strength of jute/PLA composite before and after aging

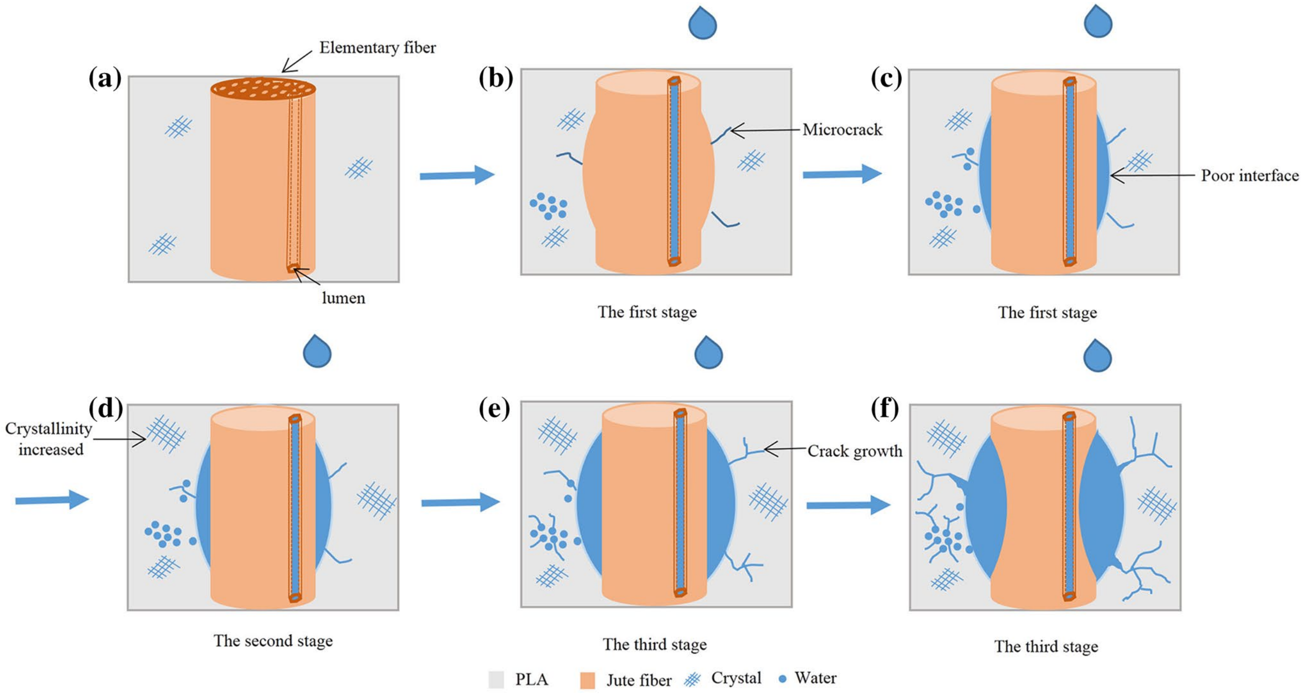

Fig. 11 Hydrothermal aging mechanism of jute/PLA composites

PLA matrix after water absorption lead to the stress and the microcracks appeared around the jute fiber in matrix showed in Fig. 11b. The interface between jute fiber and PLA matrix became worse with the immersion of water (Fig. 11c). In the second stage, as presented in Fig. 11d, the crystallinity of PLA increased. It was due to the addition of short jute fiber, which serve as nucleating agent can increase the crystallinity of PLA during aging. Finally, the degradation of PLA (Fig. 11e) and jute fiber (Fig. 11f) lead to the growth of cracks and the worse interface. The process of these three stages were relatively slow at 23 and 37.8 °C, while it was very quickly at 60 °C for the acceleration of molecular motion caused by high temperature. However, for plant fiber/PLA composites from hot press molding, in the first stage, there were exposed fibers along the sides of the hot press molded composites specimen by machined. Therefore, water ingress was easier by exposed fibers, which made interface changed faster. In the second stage, the crystallinity of PLA normally decreased after aging due to the bigger size of plant fiber, which can bring more defects to decrease the crystallinity. At last, delamination was always found, which can bring the failure of the composites. The different main failure mode between the composites from injection molding and hot press molding was due to the different aging behavior and mechanism.

Conclusions

The effect of hydrothermal aging on injection molded jute/PLA composite were investigated. The water absorption and the degradation rate of jute/PLA composite were significantly influenced by hydrothermal temperature. The aging process was very slow at a low temperature (23 and 37.8 °C in this paper) while at a high temperature (60 °C in this paper) the rate was increased. Different swelling between in matrix and jute fibers resulted in the first decline of the mechanical properties of jute/PLA composites. With the crystallinity of PLA increasing, the mechanical properties reached a stable level. The last decline in mechanical properties were mainly due to the hydrolysis of PLA matrix, which can be confirmed by GPC results. For 60 °C, the mechanical properties declined rapidly for the drastic degradation of PLA. The hydrothermal aging mechanisms of jute/PLA composites included plasticization of matrix, swelling of materials, structural damage of jute/PLA composites, change of PLA crystallinity and hydrolysis of jute fiber and PLA matrix. This study can be useful in further investigation and potential application of plant fiber reinforced composites.

Acknowledgements This work was supported by the National Basic Research Program of China (973 Project) (Grant numbers 2010CB631105), the Natural Science Foundation of China (Grant numbers 51103108 and 11172212), State Key Laboratory of Molecular Engineering of Polymers and State Key Laboratory for Strength and Vibration of Mechanical Structures (SV2017-KF-16).

References

1. Vink ETH, Rábago KR, Glassner DA, Gruber PR (2003) Polym Degrad Stab 80:403–419
2. Garlotta D (2001) J Polym Environ 9:63–84
3. Baiardo M, Frisoni G, Scandola M, Rimelen M, Lips D, Ruffieux K, Wintermantel E (2003) J Appl Polym sci 90:1731–1738
4. Pang X, Zhuang X, Tang Z, Chen X (2010) Biotechnol J 5:1125–1136
5. Lunt J (1998) Polym Degrad Stab 59:145–152
6. Amass W, Amass A, Tighe B (1998) Polym Int 47:89–144
7. Brzeziński M, Biela T (2015) Polym Int 64:1667–1675
8. Ganster J, Fink H-P, Pinnow M (2006) Compos Part A 37:1796–1804
9. Beg MDH, Pickering KL (2008) Compos Part A 39:1091–1100
10. Oever MJAVD, Beck B, Müssig J (2010) Compos Part A 41:1628–1635
11. Thwe MM, Liao K (2003) Compos Sci Technol 63:375–387
12. Joseph P, Rabello MS, Mattoso L, Joseph K, Thomas S (2002) Compos Sci Technol 62:1357–1372
13. Hu R-H, Sun M-y, Lim J-K (2010) Mater Des 31:3167–3173
14. Taib RM, Ramarad S, Ishak ZAM, Todo M (2010) Polym Compos 31:1213–1222
15. Yu T, Li Y (2014) Compos Part A 58:24–29
16. Yu T, Jiang N, Li Y (2014) Compos Part A 64:139–146
17. Gil-Castell O, Badia JD, Kittikorn T, Stromberg E, Martinez-Felipe A, Ek M, Earlsson S, Ribes-Greus A (2014) Polym Degrad Stab 108:212–222
18. Woolnough CA, Yee LH, Charlton T, Charlton T, Foster LJR (2010) Polym Int 59:658–667
19. Boubakri A, Elleuch K, Guermazi N, Ayedi H (2009) Mater Des 30:3958–3965
20. Hakkarainen M, Albertsson A-C, Karlsson S (1996) Polym Degrad Stab 52:283–291
21. De Jong S, Arias ER, Rijkers D, Van Nostrum C, Kettenes-Van den Bosch J, Hennink W (2001) Polymer 42:2795–2802
22. Andersson SR, Hakkarainen M, Inkinen S, Sodergard A, Albertsson AC (2010) Biomacromol 11:1067–1073
23. Balakrishnan H, Hassan A, Imran M, Wahit MU (2011) J Polym Environ 19:863–875
24. Gorrasi G, Pantani R (2013) Polym Degrad Stab 98:1006–1014
25. Assarar M, Scida D, El Mahi A, Poilâne C, Ayad R (2011) Mater Des 32:788–795
26. Alamri H, Low IM (2012) Polym Test 31:620–628
27. Ndazi BS, Karlsson S (2011) Express Polym Lett 5:119–131
28. Spiridon I, Leluk K, Resmerita AM, Darie RN (2015) Compos Part B Eng 69:342–349
29. Sreekumar P, Joseph K, Unnikrishnan G, Thomas S (2007) Compos Sci Technol 67:453–461
30. Almgren KM, Gamstedt EK, Berthold F, Lindström M (2010) Polym Compos 30:1809–1816
31. Almgren KM, Akerholm M, Gamstedt EK, Salmen L, Lindstrom M (2008) J Reinf Plast Comp 27:1709–1721
32. Regazzi A, Corn S, Ienny P, Bénézet J-C, Bergeret A (2016) Ind Crop Prod 84:358–365
33. Iii WVS, Billington SL (2013) Compos Part A Appl S 50:81–92
34. Li Y, Hu YP, Hu CJ, Yu YH (2008) Adv Mater Res Trans Tech Publ 33:553–558
35. Kunanopparat T, Menut P, Morel MH, Guilbert S (2008) Compos Part A Appl S 39:777–785
36. Lee S-H, Ohkita T, Kitagawa K (2004) Holzforschung 58:529–536
37. Shen CH, Springer GS (1976) J Compos Mater 10:2–20
38. Lim L-T, Auras R, Rubino M (2008) Prog Polym Sci 33:820–852
39. Huang Y, Zhang C, Pan Y, Zhou Y, Jiang L, Dan Y (2013) Polym Degrad Stab 98:943–950
40. Espert A, Vilaplana F, Karlsson S (2004) Compos Part A Appl S 35:1267–1276
41. Iii WVS, Frank CW, Billington SL (2012) Polymer 53:2152–2161
42. Zhang X, Espiritu M, Bilyk A, Kurniawan L (2008) Polym Degrad Stab 93:1964–1970
43. Yussuf A, Massoumi I, Hassan A (2010) J Polym Environ 18:422–429
44. Sombatsompop N, Chaochanchaikul K (2004) Polym Int 53:1210–1218
45. Acioli-Moura R, Sun XS (2008) Polym Eng Sci 48:829–836
46. Thuault A, Eve S, Blond D, Bréard J, Gomina M (2014) J Compos Mater 48:1699–1707